

# Early Calibration Results from the Atmospheric Infrared Sounder (AIRS) on Aqua

Thomas S. Pagano, Hartmut H. Aumann, Steven L. Gaiser, David T. Gregorich

Jet Propulsion Laboratory,  
California Institute of Technology, Pasadena, CA

## ABSTRACT

The Atmospheric Infrared Sounder (AIRS) is a space-based hyperspectral infrared instrument designed to measure Earth's atmospheric water vapor and temperature profiles on a global scale. AIRS has 2378 infrared channels in the spectral range of 3.7 – 15.4 microns with a spatial resolution of 13.5 km and 4 Vis/NIR channels from 0.4 to 0.8 microns with a spatial resolution of 2.3 km. AIRS is one of several instruments on-board the Earth Observing System (EOS) Aqua spacecraft launched May 4, 2002. AIRS has completed its Activation and Evaluation (A&E) phase and is currently in its operational mode. This paper summarizes the AIRS instrument radiometric, spatial, and spectral performance as measured in orbit during the A&E phase. Instrument noise performance, spectral alignment dependence on temperature and other factors, and spatial pointing accuracy are discussed.

Keywords: Earth Science, EOS, Aqua, AIRS, Sounder, Calibration

## 1. THE AIRS INSTRUMENT

The AIRS instrument (shown in Figure 1) incorporates numerous advances in infrared sensing technology to achieve a high level of measurement sensitivity, precision, and accuracy. This includes a temperature-controlled grating and long-wavelength cutoff HgCdTe infrared detectors cooled by an active pulse tube cryogenic cooler.

The AIRS infrared spectrometer acquired 2378 spectral samples at resolutions,  $\lambda/\Delta\lambda$ , ranging from 1086 to 1570, in three bands: 3.74  $\mu\text{m}$  to 4.61  $\mu\text{m}$ , 6.20  $\mu\text{m}$  to 8.22  $\mu\text{m}$ , and 8.8  $\mu\text{m}$  to 15.4  $\mu\text{m}$ . A cross section of the scan head assembly is shown in Figure 2. A 360-degree rotation of the scan mirror generates a scan line of IR data every 2.667 seconds.

The VIS/NIR photometer which contains four spectral bands, each with nine pixels along track, with a 0.185-degree IFOV, is boresighted to the IR spectrometer to allow simultaneous visible and infrared scene measurements.

The diffraction grating in the IR spectrometer disperses the radiation onto 17 linear arrays of HgCdTe detectors (see Figure 3) in grating orders 3 through 11. Each linear array is comprised of N elements (where N ranges from 94 to 192) by two rows (A and B) for redundancy. Gain tables in the electronics determine whether each channel uses the A side or B side detector or both. The IR spectrometer is cooled to 155 K by a two-stage passive radiative cooler.

The IR focal plane is cooled to 60 K by a Stirling/pulse tube cryocooler. The scan mirror operates at approximately 265 K due to radiative coupling to the Earth and space and to the 150-K IR spectrometer. Cooling of the IR optics and detectors is necessary to achieve the required instrument sensitivity. The VIS/NIR photometer uses optical filters to

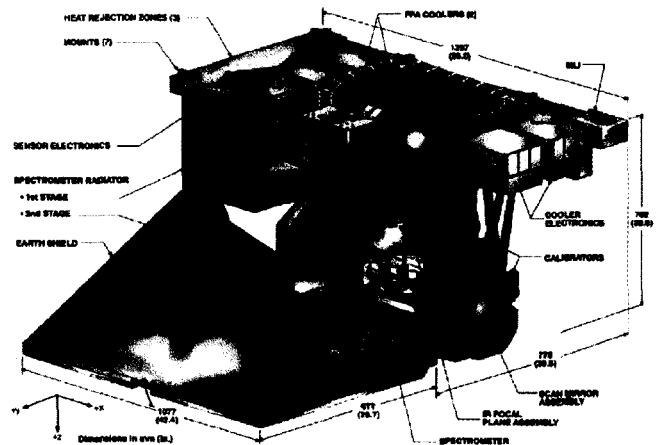


Figure 1. The Atmospheric Infrared Sounder (AIRS).

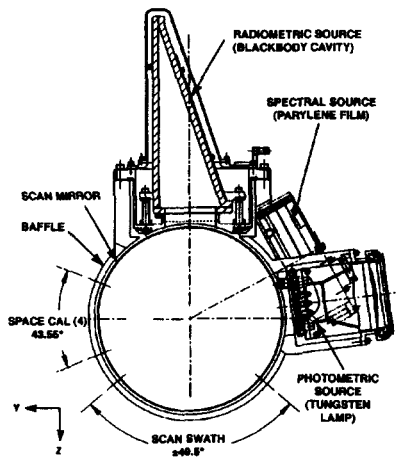


Figure 2. AIRS Scan Assembly.

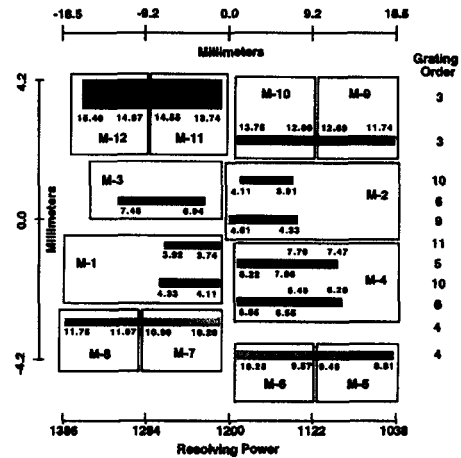


Figure 3. AIRS FPA Layout.

define four spectral bands in the 400- to 1000-nm region. The VIS/NIR detectors are not cooled and operate in the 293- to 300-K ambient temperature range of the instrument housing.

Signals from both the IR spectrometer and the VIS/NIR photometer are passed through onboard signal and data-processing electronics, which perform functions of radiation circumvention, gain ranging and DC Restore (DCR), signal integration, and output formatting and buffering to the high-rate science data bus. In addition, the AIRS instrument contains command and control electronics whose functions include communications with the satellite platform, instrument redundancy reconfiguration, the generation of timing and control signals necessary for instrument operation, and collection of instrument engineering and housekeeping data.

The Stirling/pulse tube cryocoolers are driven by separate electronics that control the phase and amplitude of the compressor moving elements to minimize vibration and to accurately control the temperature. Heat from the electronics is removed through coldplates connected to the spacecraft's heat-rejection system.

## 2. ON-ORBIT TESTS

The AIRS project has prepared an In-Flight Calibration Plan<sup>1</sup> which describes the approach used to meet the requirements of the AIRS Level 1B Algorithm Theoretical Basis Document (ATBD)<sup>2</sup>. The approach combines pre-flight calibration data, spacecraft integration and early on-orbit checkout special test results, and long term monitoring of the data to achieve the calibration. Prior papers<sup>3,4</sup>, that focused on the pre-flight calibration, have shown excellent characterization, and we will not discuss that here. A paper presented at SPIE in July of 2002<sup>5</sup> presents some results from pre-flight testing in the spacecraft and early on-orbit checkout tests. This paper presents the latest in-flight measurements for radiometric, spectral and spatial performance at the completion of the activation and evaluation phase of the mission. For more details on the procedures for these tests, see the In-Flight Calibration Plan<sup>1</sup>. For additional information on the launch operations and overall project activities at JPL, please consult the SPIE Operational Readiness paper.<sup>6</sup>

## 3. RADIOMETRIC PERFORMANCE

The AIRS radiometric performance can be categorized into radiometric accuracy and sensitivity. The radiometric accuracy is dependent on the systematic errors that result from the pre-flight calibration. The on-board calibrator (OBC) blackbody is calibrated relative to an external NIST-traceable large area blackbody using AIRS itself to make the transfer. A comprehensive assessment of the accuracy of the AIRS pre-flight radiometric calibration, and a description of the radiometric calibration approach are discussed in reference 7. Residual systematic errors for AIRS as cited in this reference are less than 0.2K at 265K for all channels.

### 3.1 In-Flight Radiometric Accuracy

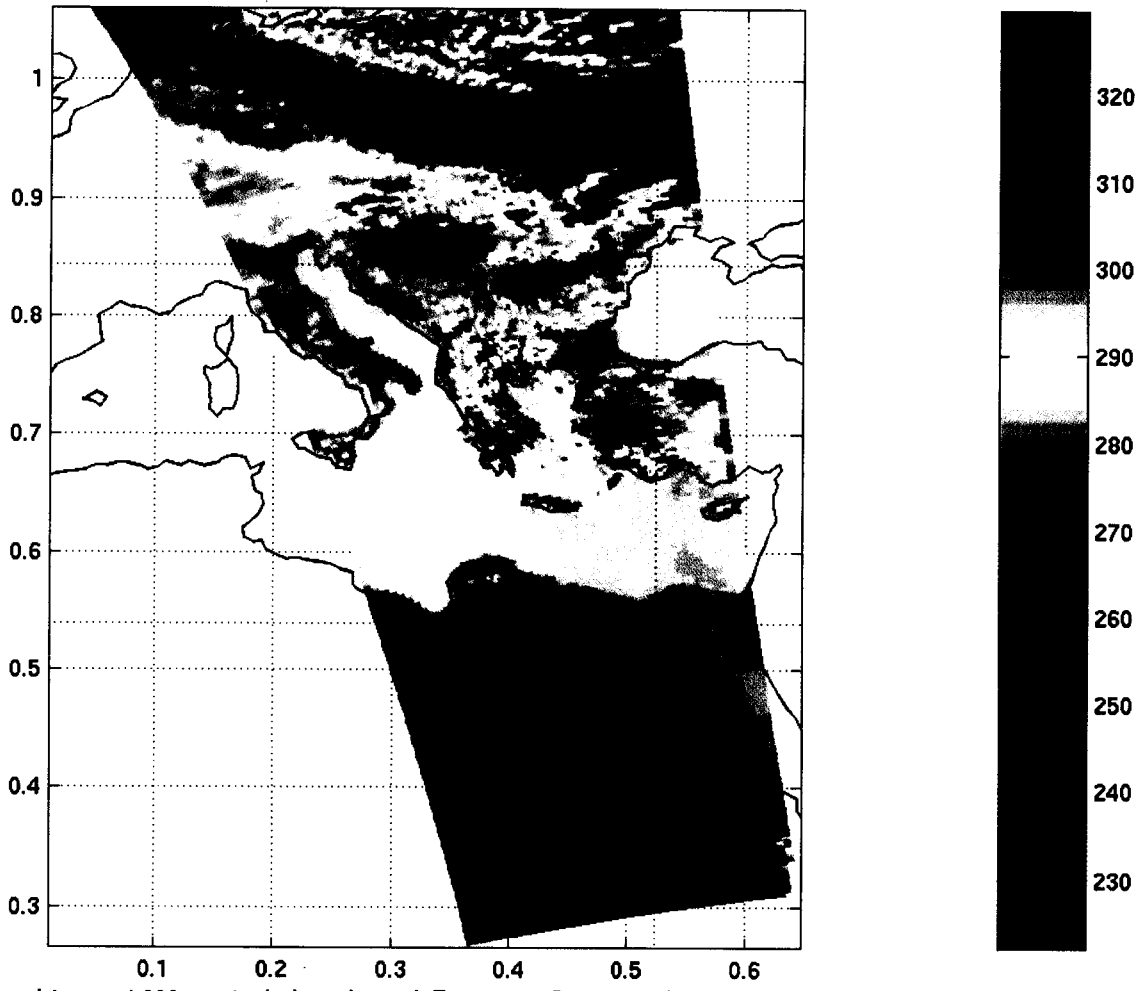
For the evaluation of radiometric accuracy of the AIRS data on-orbit we compare radiances produced by the AIRS Level 1B software with independent ground-truth under cloud-free conditions. For the early evaluation this comparison was limited to two channels at  $2616\text{cm}^{-1}$  and  $900\text{cm}^{-1}$ , where the atmosphere is highly transparent. Figure 4 shows a daytime image of the area centered on the Eastern Mediterranean based data at  $900\text{cm}^{-1}$  selected for this early evaluation. This data was taken on 14 June 2002, one day after the AIRS instrument was activated. The image shows the hot deserts of northern Africa, the moderately cool Mediterranean Sea. There is a fair amount of scattered clouds visible over Europe, with a strong cold front visible over Northeastern Europe. The Mediterranean Sea was selected for the evaluation of the radiometric accuracy because the ocean surface temperature, and temperature and moisture profiles are well known due to the wealth of available in-situ meteorological data and because the ocean area was fairly free of clouds on 14 June 2002. The median clear ocean temperature was 293K.

The radiometric analysis used data from a night over pass of the Mediterranean 12 hours earlier than the image in Figure 4. A simple spatial coherence filter, based on the analysis of a  $3 \times 3$  group of AIRS footprints, was used to identify likely clear data points. The footprint at the center is defined as "coherence clear" if its brightness temperature at  $2616\text{cm}^{-1}$  differs from that of each of the eight surrounding footprints by less than 1K. This is equivalent to requiring that the standard deviation of the brightness temperatures of the nine footprints is less than 0.35, but is computationally faster. If the field of view in the 9 footprints was perfectly uniform, then 99% of the data would pass the coherence test. The Noise Equivalent Delta Temperature (NEDT) of the  $2616\text{cm}^{-1}$  channel at 293K is about 0.15K. Only footprints with a land fraction of less than 1% were included. For this data 2684 of 4086 ocean pixels were "coherence clear". For the "clear" footprints we then corrected the surface temperature given in the NCEP analysis at the footprint location for the atmospheric transmission using the NCEP  $T(p)$ ,  $q(p)$  information and the Masuda<sup>8</sup> model for the surface emissivity.

The histogram of  $(\text{TOA.corrected .SST} - \text{AIRS.observed})$  at  $900$  and  $2616\text{cm}^{-1}$  is shown in Figure 5. We used "clear" in quotation marks because the coherence filter passes some areas with uniform overcast as "clear". These outliers are "false clear". This is the reason of the outliers visible in the histograms, some in excess of 5K. For this reason we use the median of the distribution, rather than the mean. The median of the distribution is 0.13K and 0.18K at  $900$  and  $2616\text{cm}^{-1}$ , respectively, i.e. the temperature observed by AIRS is slightly colder than the temperature in the NCEP analysis. The uncertainty in the TOA correction is 0.1K and 0.3K at  $900$  and  $2616\text{cm}^{-1}$ , respectively. Within the scope of early radiance validation and uncertainty in the TOA correction the observed small bias is negligible, and consistent with the conclusion that the absolute calibration is good to within 0.5K at 293K. However, the fact that the nighttime ocean skin temperature is typically 0.3K colder than the bulk temperature stated in the NCEP model due to evaporative cooling is likely to contribute to the observed bias. If the spatial coherence test was tightened to 0.4K, the number of pixels identified as "clear" would decrease to 1160 of 4068, with a median of 0.11K and 0.13K at  $900$  and  $2616\text{cm}^{-1}$ , respectively, i.e. the cold bias decreased by less than 0.05K. The contribution of cloud-contaminated pixel with the 1K "clear" threshold for this particular data set is thus less than 0.05K.

The method outlined above works in areas with a fairly high fraction of clear pixels, where the number of true clear pixels exceeds the number of "false clear" pixels by an order of magnitude. This is totally acceptable for the validation of the calibration. However, finding an area with 1160 of 4068, i.e. 28%, clear pixels is extremely unusual. The global data analysis for 14 June 2002 showed that only about 1% of the night ocean footprints is "clear" using the 0.4K coherence test. More recent analysis has extended the wavelength coverage for the validation of the radiometric calibration to a much wider range of frequencies<sup>9</sup>.

AIRS.2002.06.14.116.L1B.AIRS<sub>R</sub>ad.v2.3.3.2.A02165215116



btemp at 900cm<sup>-1</sup> window channel. Day pass. Ocean cooler than land!

Figure 4. Early AIRS window channel image of the Mediterranean shows excellent thermal contrast and low NEdT.

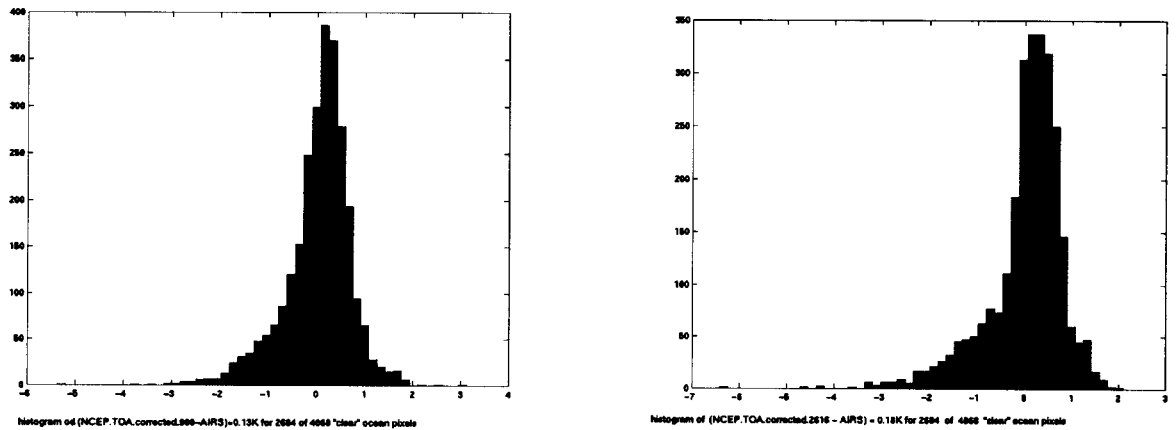


Figure 5. Histogram of apparently clear footprints show very small bias.

Left) 900 cm<sup>-1</sup>, Right) 2616 cm<sup>-1</sup>

### 3.2 Radiometric Sensitivity

Random instrumental noise limits the “Radiometric Sensitivity” of any single measurement. Sensitivity is usually expressed as the Noise Equivalent Temperature Difference (NE $\Delta$ T) and is easily measured pre-flight and in-orbit. Our method, described in more detail in reference 5, measures the instrumental noise while viewing space and the OBC blackbody, and interpolates between them to give the noise at our reference temperature; 250K. The interpolation equation<sup>5</sup> combines the noise contributions from the detector/electronics noise and the scene photon noise, calculating total noise as a function of scene radiance.

Figure 6 shows the measured rms noise for AIRS expressed as NE $\Delta$ T at 250K. The figure compares the pre-flight noise to that determined in-orbit using identical techniques. We see good agreement between the pre-flight and in-orbit measurements, indicating the instrument is operating as expected. We also see fewer outliers in the flight data. This is a consequence of an improved process for optimizing the gain tables that select the combination of A side and B side detectors to use in a given channel.

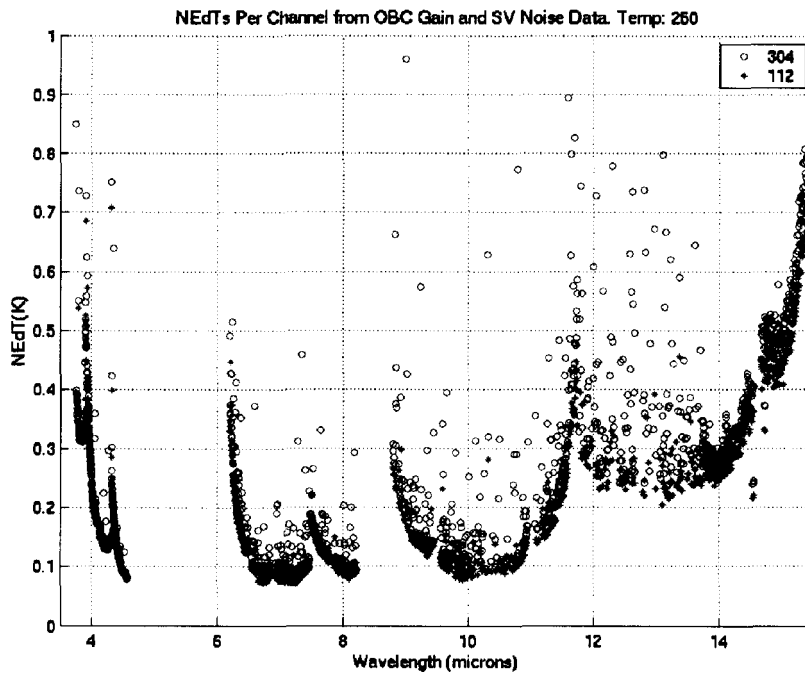


Figure 6. AIRS RMS noise expressed as NE $\Delta$ T at 250K.  
Test 304 is Pre-Flight, Test 112 is In-Orbit

The process for selecting which or both of the A side or B side detectors is used for any given channel involves careful characterization and evaluation of the noise and gain properties of each detector. The standard deviation ( $\sigma$ ) of the noise data acquired while viewing space is first calculated and called the NE $\Delta$ n. We first look at the magnitude of the NE $\Delta$ n; any detector with NE $\Delta$ n greater than 3 times the quadratic fit to the NE $\Delta$ n for the array is called noncompliant.

Also a criteria in determining the usefulness of a detector is the non-Gaussian behavior. The number of data points that are greater than 3 x NE $\Delta$ n are called 3-sigma events. We compare the number of 3-sigma events to that expected assuming Gaussian statistics with a 2x margin. We use 40,000 data points in the noise measurement, we expect 107 3-sigma events, so our threshold is 214 events. If a detector has more than 214 3-sigma events, it is called non-compliant. Effects of radiation, primarily in the South Atlantic Anomaly, are mitigated by the AIRS radiation circumvention processor discussed in the literature.<sup>5</sup>

We also look at detector “popping”. A pop is classified as any channel which has 4 events greater than 4-sigma in a row with the same sign. This is equivalent to a step in the offset. Any channel which “pops” is called non-compliant. All A and B side detectors are ranked and a selection process picks the combination that offers the optimum performance.

To illustrate the improvement achieved by the A/B selection process, Figure 7 shows the number of channels that violate the allowable number of 3 sigma events (a), and the number of pops (b) measured in orbit for A side, B side and AB optimum gain table configurations. The number of channels considered non-compliant is plotted for each of the 15 PV HgCdTe detector modules. The longest wavelength module, M10, numbered 15 in the charts, has the most offenders.

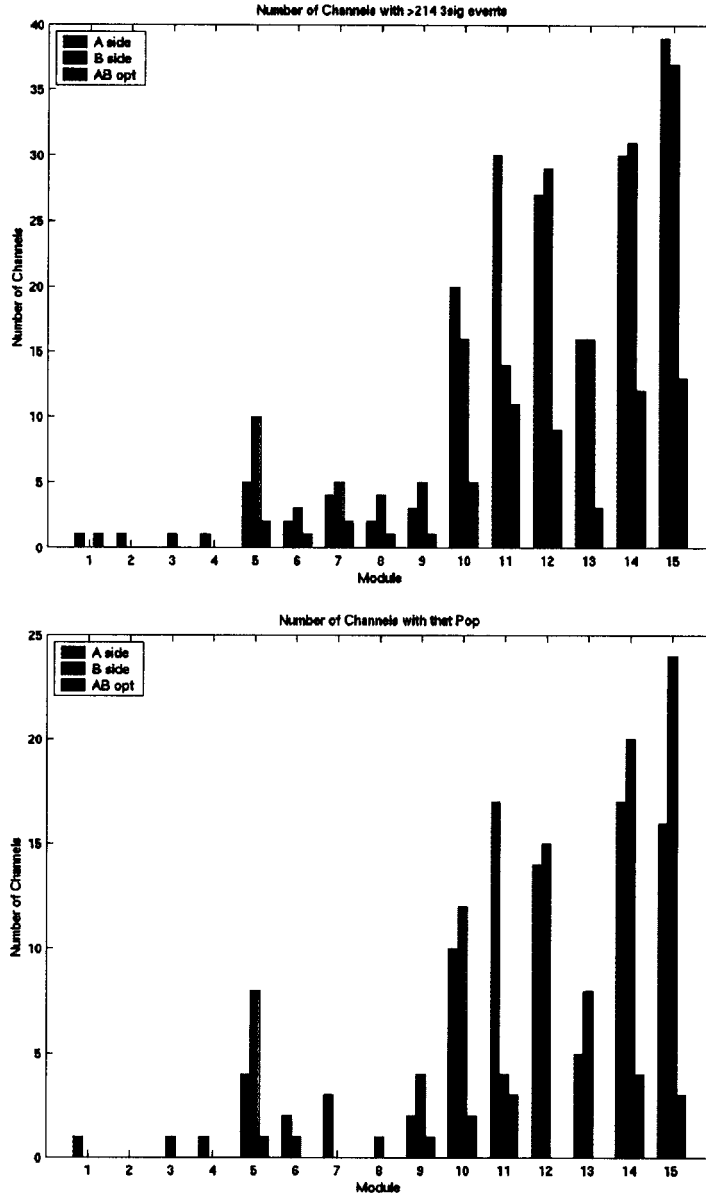


Figure 7. a) Top. Number of channels that exceed allowable number of 3 sigma events. b) Bottom. Number of channels that experience at least one pop in the 40,000 sample data set.

We believe this is due to the larger number of defects in the material and largest 1/f noise. The total number of non-compliant channels for 3-sigma events is 181, 171, and 61 for A, B and AB optimum gains respectively. Similarly the number of non-compliant channels for pops is 92, 98 and 14 for A, B and AB optimum gains respectively. After selection of A and B optimum detectors, accounting for those who have consistently high noise, less than 9% of the 2378 infrared channels have undesirable noise properties.

#### 4. SPECTRAL PERFORMANCE

AIRS in-orbit spectral calibration consists of the determination of the centroids of the Spectral Response Functions (SRFs) for each channel<sup>2</sup>. The determination of the shape of each SRF was a pre-flight activity<sup>4</sup>. Spectral centroids are determined by correlating observed radiance spectra with pre-calculated modeled radiances.

Figure 8 shows calculated focal plane position as a function of time. One micron of focal plane shift corresponds to centroid frequency shifts of one percent of each channel's full width at half maximum. Late on June 14, the spectrometer temperature was lowered, causing the observed change in calculated focal plane offset.

During stable periods, the standard deviation of individual calculations of focal plane offset is 0.25 microns. Averaging these values over the thermal time constant of the instrument, twelve hours, reduces the uncertainty in the mean shift to under 0.02 microns relative. Absolute accuracy of better than 0.5 microns, corresponding to one half of one percent of  $\Delta\nu$ , is indicated by analysis of in-orbit channel phase test results and by preliminary analysis of modeled upwelling radiance spectra.

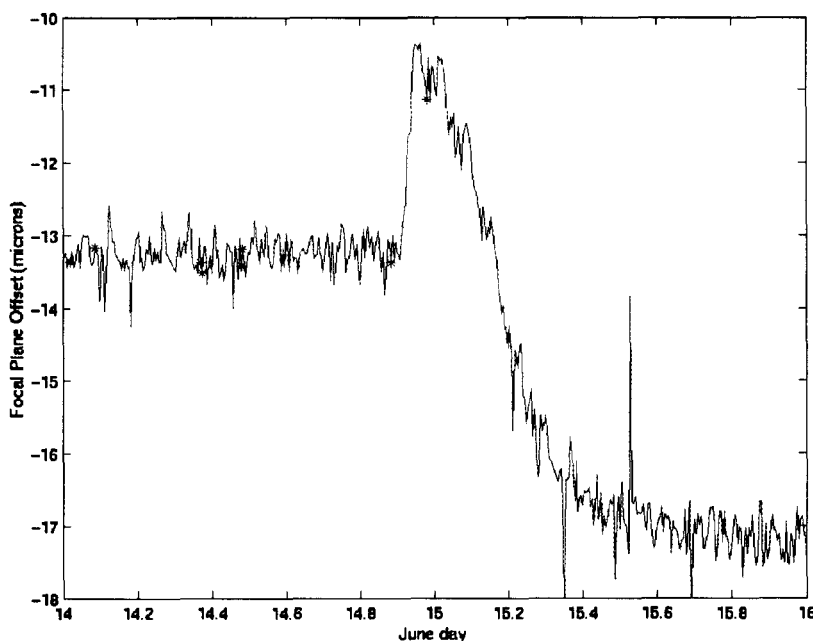


Figure 8. Calculated focal plane position vs time for AIRS is based on spectral features in the upwelling spectrum.

#### 5. SPATIAL PERFORMANCE

Determination of the boresight accuracy of the AIRS instrument beam is done using the detection of coastline crossings in one or more window channels. Optimal use of the AIRS IR data with data from the on-board microwave instruments requires the AIRS boresight to be known to about 2 km, which is a fraction of the effective nadir footprint of 13.5 km. Use with the AIRS visible channels for cloud flagging requires knowledge of the boresight to about half the visible field of view or about 1.3 km. The coastline detection scheme is described elsewhere<sup>11</sup>.

The results of the analysis of several days of initial data from the instrument are shown in Figures 9. This data, from the window channel at  $2616\text{ cm}^{-1}$ , was obtained from moderately clear, globally distributed locations. The data was processed in both the scan and track directions to attempt to account for changing coastline directions. In both cases the mean differences are within the specifications described above. The scatter in the data is probably due in large part to cloud contamination from choosing areas that were only moderately clear, since in this initial analysis we could only find a few very clear homogeneous regions.

**Table 1. Measured Latitude and Longitude errors on Scan and Track boresight positions.**

	Lat diff s	Lon diff s	Lat diff t	Lon diff t
Mean	0.5918	0.8431	-0.3804	0.5072
Std. Dev	2.7515	3.6836	2.3950	4.2506
Std. Dev Mean	0.4196	0.5617	0.3652	0.6482

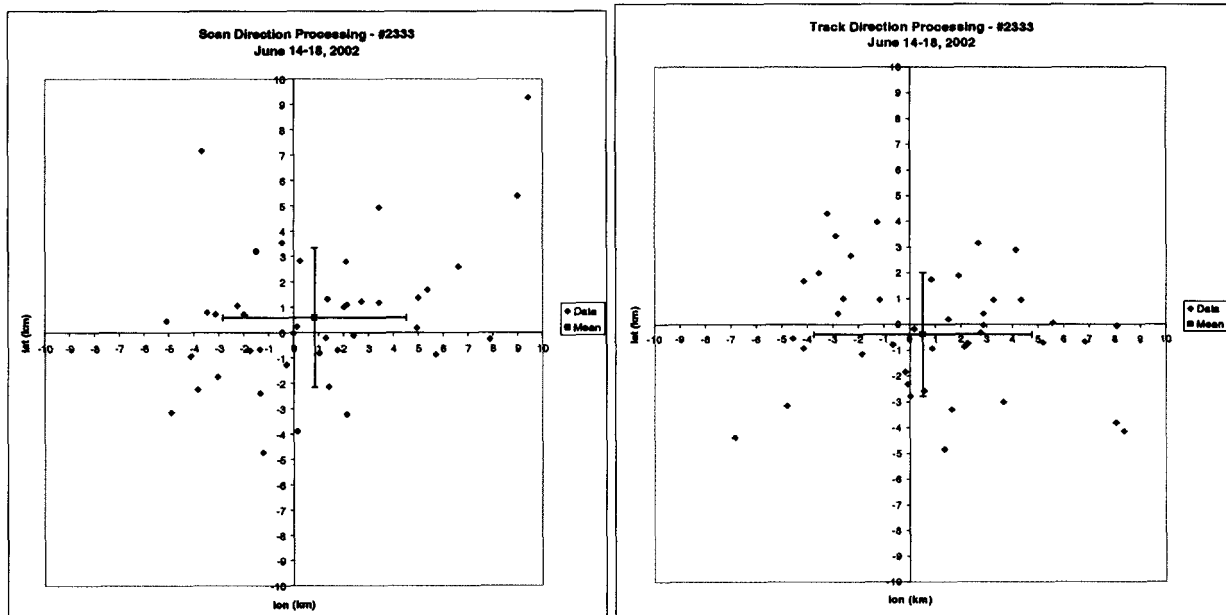


**Figure 9. Scan (left) and Track (right) pointing errors for AIRS measured from coastline crossings.**

### ACKNOWLEDGEMENTS

The authors would like to thank the other members of the AIRS Calibration Team at JPL who participated in the analyses presented in this paper including Steve Broberg, Steve Licata and, Thomas Hearty, and the ACT members at BAE SYSTEMS including Ken Overoye and Margie Weiler. This research was carried out at the Jet Propulsion Laboratory, California Institute of Technology, under a contract with the National Aeronautics and Space Administration.

### REFERENCES

1. T. Pagano, Editor, "The Atmospheric Infrared Sounder (AIRS) Visible and Infrared In-Flight Calibration Plan, Version 3.0, June 2002, JPL-D-18816. Available at [www.jpl.nasa.gov/airs](http://www.jpl.nasa.gov/airs)
2. "AIRS Level 1b Algorithm Theoretical Basis Document (ATBD) Part 1 (IR), Version 2.2," H. Aumann et al., November 10, 2000, <http://eospsqsti.nasa.gov/atbd/airstables/html>
3. P. Morse, J. Bates, C. Miller, "Development and test of the Atmospheric Infrared Sounder (AIRS) for the NASA Earth Observing System (EOS).", SPIE 3759-27, July 1999.

4. T. Pagano et al., "Pre-launch Performance Characteristics of the Atmospheric Infrared Sounder (AIRS)", SPIE 4169-41, September 2000.
5. T. Pagano et al., "On-Board Calibration Techniques and Test Results for the Atmospheric Infrared Sounder (AIRS)", SPIE 4814-38, July 2002
6. T. Pagano et al., "Operational Readiness for the Atmospheric Infrared Sounder (AIRS) on the Earth Observing System Aqua spacecraft", SPIE 4483-04, August 2001
7. T. Pagano et al., "Pre-Launch and In-Flight Radiometric Calibration of the Atmospheric Infrared Sounder (AIRS)", IEEE TGRS-00136-2002, to be published.
8. Masuda, K., T. Takashima and Y. Takayama, "Emissivity of pure and sea waters for the model sea surface in infrared window regions", Remote Sensing of the Environment, 24, 313-329 (1988)
9. Aumann H. H. and T.S. Pagano, "Early Results from the Advanced Infrared Temperature Sounder (AIRS) on the EOS Aqua", Proc. SPIE Europto 23 September 2002, Crete, Greece.
10. S. Gaiser, et. al., "In-flight Spectral Calibration of the Atmospheric Infrared Sounder", IEEE TGRS-00152-2002, to be published
11. Gregorich, D.T. et. al., "Verification of AIRS boresight accuracy using coastline detection", IEEE TGRS-00140-2002, to be published